Second-harmonic polarizability including electron-hole attraction from band-structure theory

R. Leitsmann,* W. G. Schmidt, P. H. Hahn, and F. Bechstedt
Institut für Festkörpertheorie und -optik, Max-Wien-Platz 1, 07743 Jena, Germany
(Received 12 January 2005; revised manuscript received 2 March 2005; published 31 May 2005)

We revisit the derivation of the expressions for the calculation of second-harmonic generation spectra and show the equivalence of different approaches proposed in the literature. A method is suggested to include excitonic effects in the calculation. Numerical tests are performed for the linear and nonlinear optical response of bulk GaAs. Excitonic effects are found to give rise to a redistribution of oscillator strength, thus improving the agreement with experiment.

DOI: 10.1103/PhysRevB.71.195209 PACS number(s): 78.20.Bh, 71.10.−w, 42.70.Nq

I. INTRODUCTION

Linear and nonlinear methods of optical spectroscopy are rapidly gaining importance for materials characterization.[1–3] Even-order nonlinear optical spectroscopy has emerged as an unusually sensitive technique for noninvasive analysis of surfaces and buried interfaces of centrosymmetric materials.[4] In order to fully exploit the diagnostic potential of such spectroscopies and in order to assist in the development of novel optical materials, methods are required to predict the magnitude and frequency dependence of linear and nonlinear optical susceptibilities with high accuracy. Recent years have seen impressive methodological progress in the accurate numerical modeling of linear optical properties from *first-principles*.

The typical starting point is the independent-(quasi)particle approximation (IPA/IQA) in which the linear dielectric function (for translationally invariant systems) is given by

$$\epsilon_{\alpha\beta}(\omega) = \delta_{\alpha\beta} + \frac{8\pi e^2}{\hbar m^2 \tilde{\omega}^2 V} \sum_{nm\mathbf{k}} f_{nm}(\mathbf{k}) \frac{p^{\alpha}_{nm}(\mathbf{k}) p^{\beta}_{mn}(\mathbf{k})}{\omega_{mn}(\mathbf{k}) - \tilde{\omega}}. \quad (1)$$

Here the $f_{nm}(\mathbf{k}) = f(\epsilon_n(\mathbf{k})) - f(\epsilon_m(\mathbf{k}))$ are the Fermi blocking factors for the Bloch states $|n\mathbf{k}\rangle$ and $|m\mathbf{k}\rangle$ with the energies $\epsilon_n(\mathbf{k})$ and $\epsilon_m(\mathbf{k})$, V is the system volume, and $\tilde{\omega} = \omega + i\eta$ is the frequency with a small positive imaginary part η, which turns off the electromagnetic field adiabatically. The

$$p^{\alpha}_{nm} = \langle n\mathbf{k}|\hat{p}^{\alpha}|m\mathbf{k}\rangle \quad (2)$$

are the momentum matrix elements of the system and $\hbar w_{mn}(\mathbf{k}) = \epsilon_m(\mathbf{k}) - \epsilon_n(\mathbf{k})$ are the energy differences between band m and n at point $\mathbf{k}$ in the Brillouin zone (BZ). These values can be calculated, e.g., within density-functional theory in the local-density approximation (DFT-LDA). Additionally, self-energy effects can be included in the *GW* approximation.[5–7] Moreover, the Bethe-Salpeter equation (BSE) can be solved for pair excitations in order to account for excitonic and local-field (LF) contributions to the linear optical response.[8–10] Linear optical properties can thus be predicted reliably even for complex systems such as semiconducter surfaces[11,12] or water.[13]

The progress in the numerical determination of nonlinear optical susceptibilities, however, is lagging behind. The formalism is far more complex. Therefore, different numerical and methodological approaches for the *ab initio* calculation of the nonlinear optical response are used,[14–16] which are not easily seen to be equivalent. Numerical results obtained within the IQA for the second-harmonic susceptibility $\chi^{(2)}_{xyz}(-2\omega;\omega,\omega)$, even of simple bulk systems such as GaAs,[15,17–19] neither agree very well with each other nor with the experiment.[20] Numerical results including electron-hole interaction are presently available only for low photon frequencies.[21] Due to these deficiencies in the numerical modeling of second-harmonic generation (SHG) spectra from *first-principles*, empirical and semiempirical approaches[22,23] are still widely used for their interpretation.

The deficiencies in the theoretical description and numerical calculation of SHG spectra motivate the present study. We start with a brief review of the methodology to calculate response functions from band-structure theory. For the SHG case, the equivalence to Aspnes' approach[16] as well as to the derivation by Sipe *et al.*[17] is shown. Then a method is proposed to include excitonic and local-field effects in nonlinear-response functions. Finally, numerical results for the prototypical example of bulk GaAs are presented. Both linear and nonlinear optical responses are discussed, to allow for a better understanding of the physics behind the many-body interactions.

II. THEORY

A. Time-dependent perturbation theory

Within the interaction picture, the time evolution operator is given by

$$\hat{U}(t) = 1 - \frac{i}{\hbar}\int_{-\infty}^{t} \mathrm{d}t' \hat{H}^{\mathrm{ext}}(t')\hat{U}(t'), \quad (3)$$

with the external perturbation Hamiltonian in minimum coupling convention

$$\hat{H}^{\mathrm{ext}}(t) = -\frac{1}{c}\int d^3\mathbf{x}\hat{\mathbf{j}}^{\mathrm{dyn}}(\mathbf{x},t)\mathbf{A}^{\mathrm{ext}}(\mathbf{x},t) - \frac{e^2}{2mc^2}\int d^3\mathbf{x}\hat{\rho}(\mathbf{x},t) \times[\mathbf{A}^{\mathrm{ext}}(\mathbf{x},t)]^2, \tag{4}$$

where

$$\hat{\mathbf{j}}^{\mathrm{dyn}}(\mathbf{x},t) = \frac{e}{2m}[\hat{\Psi}^\dagger(\mathbf{x},t)[\hat{\mathbf{p}}\hat{\Psi}(\mathbf{x},t)] - [\hat{\mathbf{p}}\hat{\Psi}^\dagger(\mathbf{x},t)]\hat{\Psi}(\mathbf{x},t)] \tag{5}$$

is the dynamical current density operator and $\mathbf{A}^{\mathrm{ext}}$ represents the vector potential of the external electromagnetic field. The total current density operator

$$\hat{\mathbf{j}}(\mathbf{x},t) = \hat{\mathbf{j}}^{\mathrm{dyn}}(\mathbf{x},t) - \frac{e^2}{mc}\hat{\rho}(\mathbf{x},t)\mathbf{A}^{\mathrm{ext}}(\mathbf{x},t) \tag{6}$$

can be obtained by replacing the mechanical by the electrodynamical momentum operator.

We restrict ourselves to insulators and undoped semiconductors. Then, the free-carrier density vanishes at zero temperature. Consequently, we neglect terms proportional to expectation values of the electron density operator in Eq. (4).

Exploiting gauge invariance,[48] we set

$$\varphi^{\mathrm{ext}}(\mathbf{x},t) = 0, \tag{7}$$

$$\mathbf{E}^{\mathrm{ext}}(\mathbf{x},t) = -\frac{1}{c}\partial_t\mathbf{A}^{\mathrm{ext}}(\mathbf{x},t), \tag{8}$$

$$\mathbf{B}^{\mathrm{ext}}(\mathbf{x},t) = \boldsymbol{\nabla}\times\mathbf{A}^{\mathrm{ext}}(\mathbf{x},t) \tag{9}$$

according to the transversal gauge. Here φ^{ext} is the scalar potential, $\mathbf{E}^{\mathrm{ext}}$ is the external electric field, and B^{ext} is the external magnetic field. To describe the response, we start from the relation between induced and total current density operators,

$$\hat{\mathbf{j}}^{\mathrm{ind}(\mathbf{x},t)} = \hat{U}^\dagger(t)\hat{\mathbf{j}}(\mathbf{x},t)\hat{U}(t) - \hat{\mathbf{j}}^{\mathrm{dyn}}(\mathbf{x},t), \tag{10}$$

and expand the former in a power series of the vector potential $\mathbf{A}^{\mathrm{ext}}$. By expanding Eq. (3) as

$$\hat{U}(t) = 1 - \frac{i}{\hbar}\int_{-\infty}^{t}\mathrm{d}t'\hat{H}^{\mathrm{ext}}(t') - \frac{1}{\hbar^2}\int_{-\infty}^{t}\mathrm{d}t'\int_{-\infty}^{t'}\mathrm{d}t''\hat{H}^{\mathrm{ext}}(t')\hat{H}^{\mathrm{ext}}(t'') + \cdots, \tag{11}$$

one obtains from Eq. (4) (without terms proportional to the free-carrier density)

$$\hat{\mathbf{j}}^{\mathrm{ind}}(\mathbf{x},t) = \sum_{i=1}^{\infty}\hat{\mathbf{j}}^{\mathrm{ind(i)}}(\mathbf{x},t), \tag{12}$$

with

$$\hat{j}_\alpha^{\mathrm{ind}(1)}(\mathbf{x},t) = -\frac{i}{\hbar c}\int \mathrm{d}^3x'\int_{-\infty}^{t}\mathrm{d}t' \times[\hat{j}_\beta^{\mathrm{dyn}}(\mathbf{x}',t'),\hat{j}_\alpha^{\mathrm{dyn}}(\mathbf{x},t)]A_\beta^{\mathrm{ext}}(\mathbf{x}',t') \tag{13}$$

$$\hat{j}_\alpha^{\mathrm{ind}(2)}(\mathbf{x},t) = -\frac{1}{\hbar^2c^2}\int \mathrm{d}^3x'\int \mathrm{d}^3x''\int_{-\infty}^{t}\mathrm{d}t'\int_{-\infty}^{t'}\mathrm{d}t'' \times[\hat{j}_\gamma^{\mathrm{dyn}}(\mathbf{x}'',t''),[\hat{j}_\beta^{\mathrm{dyn}}(\mathbf{x}',t'),\hat{j}_\alpha^{\mathrm{dyn}}(\mathbf{x},t)]] \times A_\gamma^{\mathrm{ext}}(\mathbf{x}'',t'')A_\beta^{\mathrm{ext}}(\mathbf{x}',t'). \tag{14}$$

The corresponding expectation values for nonmagnetic materials are given by

$$\langle\hat{j}_\alpha^{\mathrm{ind}(1)}(\mathbf{x},t)\rangle = \sum_\beta\int \mathrm{d}^3\mathbf{x}'\int_{-\infty}^{\infty}\mathrm{d}t' \times\tilde{\sigma}_{\alpha\beta}^{(1)}(\mathbf{x},\mathbf{x}',t-t')E_\beta^{\mathrm{ext}}(\mathbf{x}',t'), \tag{15}$$

$$\langle\hat{j}_\alpha^{\mathrm{ind}(2)}(\mathbf{x},t)\rangle = \sum_{\beta\gamma}\int \mathrm{d}^3\mathbf{x}'\int \mathrm{d}^3\mathbf{x}''\int_{-\infty}^{\infty}\mathrm{d}t'\int_{-\infty}^{\infty}\mathrm{d}t'' \times\tilde{\sigma}_{\alpha\beta\gamma}^{(2)}(\mathbf{x},\mathbf{x}',\mathbf{x}'',t-t',t-t'')E_\beta^{\mathrm{ext}}(\mathbf{x}',t') \times E_\gamma^{\mathrm{ext}}(\mathbf{x}'',t''), \tag{16}$$

where $\tilde{\sigma}^{(i)}$ are the quasiconductivity tensors. This is in contrast to the conductivity tensors $\sigma^{(i)}$ that are related to an expansion with respect to the total electic field $\mathbf{E}(x,t)=\mathbf{E}^{\mathrm{ind}}(x,t)+\mathbf{E}^{\mathrm{ext}}(x,t)$. One can interpret the induced electric field as a field generated by the redistribution of the system electrons in the presence of the external perturbation. Within the self-consistent-field approximation, this effect is already contained in the Hamiltonian via the density-dependent self-consistent potential.[24] However, it can be shown that this effect can account for restricting the calculation of the conductivities to terms containing irreducible graphs,[49] the so called irreducible part of the expectation value.[25–28] Therefore, it holds that

$$\tilde{\sigma}^{(i)}|_{\mathrm{irred}} \to \sigma^{(i)}.$$

Taking into account that the electric fields E_β^{ext} and E_γ^{ext} are physically equivalent, the conductivity tensors are given by

$$\sigma_{\alpha\beta}^{(1)}(\mathbf{x},\mathbf{x}',t-t') = \Theta(t-t') \times\frac{1}{i\hbar}\int_t^{t'}\mathrm{d}t''\langle[\hat{j}_\beta^{\mathrm{dyn}}(\mathbf{x}',t''),\hat{j}_\alpha^{\mathrm{dyn}}(\mathbf{x},t)]\rangle_{\mathrm{irred}} \tag{17}$$

and

$$\sigma^{(2)}_{\alpha\beta\gamma}(\mathbf{x},\mathbf{x}',\mathbf{x}'',t-t',t-t'') = -\frac{1}{2\hbar^2}\int_{-\infty}^{t} \mathrm{d}t''' \times \int_{-\infty}^{t'''} \mathrm{d}t''''\Theta(t'''-t')\Theta(t'''-t'') \times\{\langle[\hat{j}^{\mathrm{dyn}}_{\gamma}(\mathbf{x}',t''''),[\hat{j}^{\mathrm{dyn}}_{\beta}(\mathbf{x}'',t'''),\hat{j}^{\mathrm{dyn}}_{\alpha}(\mathbf{x},t)]]\rangle_{\mathrm{irred}} + (\beta\leftrightarrow\gamma)\}. \quad (18)$$

B. Response functions

In general, the Fourier transforms of the response functions are wave-vector-dependent. However, here we are interested in the response to electromagnetic waves with photon energies below 10 eV. The corresponding photon wave vectors are small compared to the extent of the BZ. Therefore, the following discussion is restricted to the optical limit, i.e., vanishing wave vectors $\mathbf{q}\rightarrow\mathbf{0}$.

There is another complication related to the difference between macroscopic and microscopic optical susceptibilities, i.e., the so-called local-field (LF) effects.[26] In the case of the linear response, these effects can be treated according to the prescription of Adler and Wiser.[29,30] The effect of local fields can also be taken into account by an electron-hole exchange term in the two-particle Hamiltonian.[12,31] Such a treatment of LF effects by an additional unscreened but short-ranged Coulomb interaction between optically excited (quasi)electrons and (quasi)holes can be used in the calculation of nonlinear optical coefficients. For that reason, we follow this method for the inculsion of LF effects. Of course, studying the limit of independent (quasi)particles below, we neglect the influence of these effects by neglecting the total (quasi)electron-(quasi)hole interaction.

Within these approximations, the optical polarization $P_{\alpha}(\omega)$ can be expressed in terms of the total macroscopic electric field $\mathbf{E}(\omega)$,[32,33]

$$P_{\alpha}(\omega) = \chi^{(1)}_{\alpha\beta}(-\omega,\omega)E^{\beta}(\omega) + \chi^{(2)}_{\alpha\beta\gamma}(-\omega'-\omega'',\omega'+\omega'') \times E^{\beta}(\omega')E^{\gamma}(\omega'') + \cdots . \quad (19)$$

For nonmagnetic materials, one obtains from Maxwell's equations

$$\langle\hat{j}^{\mathrm{ind}}_{\alpha}\rangle = \frac{\partial}{\partial t}P_{\alpha}(t). \quad (20)$$

In combination with Eqs. (15) and (17), this leads to the linear dielectric function

$$\epsilon_{\alpha\beta}(\omega) = \delta_{\alpha\beta} + \frac{4\pi i}{\tilde{\omega}}\sigma^{(1)}_{\alpha\beta}(0,0,\omega) = \delta_{\alpha\beta} + \frac{4\pi i}{\hbar\tilde{\omega}^2 V}\int_0^{\infty}\mathrm{d}t e^{i\tilde{\omega}t}\langle[\hat{J}_{\alpha}(0),\hat{J}_{\beta}(-t)]\rangle_{\mathrm{irred}}, \quad (21)$$

and with Eqs. (16) and (18) to the SHG susceptibility

$$\chi^{(2)}_{\alpha\beta\gamma}(-2\omega;\omega,\omega) = i\frac{\sigma^{(2)}(0,0,0,\tilde{\omega},\tilde{\omega})}{2\tilde{\omega}} = \frac{i}{4V\hbar^2\tilde{\omega}^3}\int_{-\infty}^{0}\mathrm{d}t'\int_{-\infty}^{t'}\mathrm{d}t'' \times\{e^{-i\tilde{\omega}t'}e^{-i\tilde{\omega}t''}\langle[\hat{J}_{\gamma}(t''),[\hat{J}_{\beta}(t'),\hat{J}_{\alpha}(0)]]\rangle_{\mathrm{irred}} + (\beta\leftrightarrow\gamma)\}. \quad (22)$$

The current operators are defined by

$$\hat{J}_{\alpha}(t) = \int \mathrm{d}^3\mathbf{x}\hat{j}^{\mathrm{dyn}}_{\alpha}(\mathbf{x},t). \quad (23)$$

Using a Bloch representation,

$$\hat{J}_{\alpha}(t) = \frac{e}{m}\sum_{nm\mathbf{k}} p^{\alpha}_{nm}(\mathbf{k})\hat{a}^{\dagger}_{n\mathbf{k}}(t)\hat{a}_{m\mathbf{k}}(t), \quad (24)$$

where $\hat{a}^{\dagger}_{n\mathbf{k}}(t)$, $\hat{a}_{n\mathbf{k}}(t)$ are the creation and annihilation operators of electrons in Bloch states $|n\mathbf{k}\rangle$, one obtains the following expressions for the linear and nonlinear (here: SHG) response functions:

$$\epsilon_{\alpha\beta}(\omega) = \delta_{\alpha\beta} + \frac{4\pi i e^2}{Vm^2\hbar\tilde{\omega}^2}\sum_{\substack{nm\mathbf{k}\\ n'm'\mathbf{k}'}}\int_0^{\infty}\mathrm{d}t e^{i\tilde{\omega}t}p^{\alpha}_{nm}(\mathbf{k})p^{\beta}_{n'm'}(\mathbf{k}') \times\langle[\hat{a}^{+}_{n\mathbf{k}}(t)\hat{a}_{m\mathbf{k}}(t),\hat{a}^{+}_{n'\mathbf{k}'}(0)\hat{a}_{m'\mathbf{k}'}(0)]\rangle_{\mathrm{irred}}, \quad (25)$$

$$\chi^{(2)}_{\alpha\beta\gamma}(-2\omega;\omega,\omega) = \frac{ie^3}{4\hbar^2m^3\tilde{\omega}^3V}\sum_{\mathbf{k}\mathbf{k}'\mathbf{k}''}\sum_{nlm}\sum_{n'l'm'}p^{\gamma}_{nn'}(\mathbf{k})p^{\beta}_{ll'}(\mathbf{k}') \times p^{\alpha}_{mm'}(\mathbf{k}'')\int_{-\infty}^{0}\mathrm{d}t'\int_{-\infty}^{t'}\mathrm{d}t'' \times\{e^{-i\tilde{\omega}t'}e^{-i\tilde{\omega}t''}\langle[\hat{a}^{+}_{n\mathbf{k}}(t'')\hat{a}_{n'\mathbf{k}}(t''), \times[\hat{a}^{+}_{l\mathbf{k}'}(t')\hat{a}_{l'\mathbf{k}'}(t'),\hat{a}^{+}_{m\mathbf{k}''}(0)\hat{a}_{m'\mathbf{k}''}(0)]]\rangle_{\mathrm{irred}} + (\beta\leftrightarrow\gamma)\}. \quad (26)$$

So far, except for the restriction to one class of diagrams, no assumptions have been made about the electron-electron interaction. It will be specified in the following.

C. Independent-(quasi)particle approach

The DFT-LDA eigenvalues may be interpreted as zero-order terms of a perturbative expansion of the quasiparticle energy, which can be corrected for self-energy effects by performing quasiparticle calculations, e.g., in the *GW* approximation (GWA),[5,6,34] or by simply shifting the unoccupied state energies by a constant value, i.e., by applying the so-called scissors operator. In any case, the momentum matrix elements have to be renormalized.[7] With $\epsilon_n(\mathbf{k})$ representing the energy of state $|n\mathbf{k}\rangle$, the time dependence of the creation and annihilation operators is given by

$$\hat{a}^{\pm}_{n\mathbf{k}}(t) = e^{\pm(i/\hbar)\epsilon_n(\mathbf{k})t}\hat{a}^{\pm}_{n\mathbf{k}}. \tag{27}$$

Together with the interband energies $\hbar\omega_{nm}(\mathbf{k})$ and accounting for spin degeneracy, the response functions take the explicit forms

$$\epsilon_{\alpha\beta}(\omega) = \delta_{\alpha\beta} + \frac{8\pi e^2}{\hbar m^2\tilde{\omega}^2 V}\sum_{nm\mathbf{k}} f_{nm}(\mathbf{k})\frac{p^{\alpha}_{nm}(\mathbf{k})p^{\beta}_{mn}(\mathbf{k})}{\omega_{mn}(\mathbf{k}) - \tilde{\omega}} \tag{28}$$

and

$$\chi^{(2)}_{\alpha\beta\gamma}(-2\omega,\omega,\omega) = \frac{-ie^3}{\tilde{\omega}^3\hbar^2 m^3 V}\sum_{\mathbf{k}}\sum_{nml}\frac{1}{[\omega_{mn}(\mathbf{k}) - 2\tilde{\omega}]} \times\left[\frac{f_{nl}(\mathbf{k})p^{\alpha}_{nm}(\mathbf{k})\{p^{\beta}_{ml}(\mathbf{k})p^{\gamma}_{ln}(\mathbf{k})\}}{\omega_{ln}(\mathbf{k}) - \tilde{\omega}} + \frac{f_{ml}(\mathbf{k})p^{\alpha}_{nm}(\mathbf{k})\{p^{\gamma}_{ml}(\mathbf{k})p^{\beta}_{ln}(\mathbf{k})\}}{\omega_{ml}(\mathbf{k}) - \tilde{\omega}}\right], \tag{29}$$

where

$$\{p^{\beta}_{ml}(\mathbf{k})p^{\gamma}_{ln}(\mathbf{k})\} = \frac{1}{2}[p^{\beta}_{ml}(\mathbf{k})p^{\gamma}_{ln}(\mathbf{k}) + p^{\gamma}_{ml}(\mathbf{k})p^{\beta}_{ln}(\mathbf{k})]. \tag{30}$$

Equation (29) can be split into two- and three-band contributions. Replacing $\tilde{\omega}^3$ in the prefactor by energy differences as explained in 35, one finds

$$\chi^{(2)\,\mathrm{two}}_{\alpha\beta\gamma}(-2\omega,\omega,\omega) = -\frac{ie^3}{m^3\hbar^2 V}\sum_{nm}\sum_{\mathbf{k}}\left[\frac{16 f_{nm}(\mathbf{k})p^{\alpha}_{nm}(\mathbf{k})\{\Delta^{\beta}_{mn}(\mathbf{k})p^{\gamma}_{mn}(\mathbf{k})\}}{[\omega_{mn}(\mathbf{k})]^4[\omega_{mn}(\mathbf{k}) - 2\tilde{\omega}]} - \frac{f_{nm}(\mathbf{k})p^{\alpha}_{nm}(\mathbf{k})\{\Delta^{\beta}_{mn}(\mathbf{k})p^{\gamma}_{mn}(\mathbf{k})\}}{[\omega_{mn}(\mathbf{k})]^4[\omega_{mn}(\mathbf{k}) - \tilde{\omega}]}\right], \tag{31}$$

$$\chi^{(2)\,\mathrm{three}}_{\alpha\beta\gamma}(-2\omega,\omega,\omega) = -\frac{ie^3}{m^3\hbar^2 V}\sum_{\mathbf{k}}{\sum_{nml}}'\frac{p^{\alpha}_{nm}(\mathbf{k})\{p^{\beta}_{ml}(\mathbf{k})p^{\gamma}_{ln}(\mathbf{k})\}}{\omega_{ln}(\mathbf{k}) - \omega_{ml}(\mathbf{k})} \times\left[\frac{16 f_{nm}(\mathbf{k})}{[\omega_{mn}(\mathbf{k})]^3[\omega_{mn}(\mathbf{k}) - 2\tilde{\omega}]} + \frac{f_{ml}(\mathbf{k})}{[\omega_{ml}(\mathbf{k})]^3[\omega_{ml}(\mathbf{k}) - \tilde{\omega}]} + \frac{f_{ln}(\mathbf{k})}{[\omega_{ln}(\mathbf{k})]^3[\omega_{ln}(\mathbf{k}) - \tilde{\omega}]}\right], \tag{32}$$

where $\Delta^{\beta}_{mn} = p^{\beta}_{mm}(\mathbf{k}) - p^{\beta}_{nn}(\mathbf{k})$. The prime at the sum symbolizes that the sum runs over indices $n \neq m \neq l$. We mention that the replacement of the $\tilde{\omega}^3$ prefactor by energy differences is exact only for undoped semiconductors at zero temperature. This can easily be seen for the imaginary part of the response function.[35] For the linear case, it has been shown that this replacement corresponds to the gauge invariance of the response functions.[50] As shown in Appendix A, formulas (31) and (32) are equivalent to the corresponding expressions derived by Sipe, Ghahramani, and Hughes.[14,17] Appendix A also shows that our derivation allows a more condensed formulation of the final result for the second-order coefficients. The Bloch representation (24) includes both intraband and interband terms, without further discrimination. In the intraband case, the momentum matrix elements take the simple form

$$p^{\alpha}_{nn}(\mathbf{k}) = \frac{m}{\hbar}\frac{\partial}{\partial k_{\alpha}}\epsilon_n(\mathbf{k}). \tag{33}$$

The numerical calculations take advantage from exploiting symmetry properties. Time-reversal symmetry requires for the transition matrix elements

$$p^{\alpha}_{nm}(\mathbf{k}) = -p^{\alpha}_{mn}(-\mathbf{k}), \tag{34}$$

whereas the occupation numbers and band energies are invariant with respect to an inversion in the reciprocal space. This results in

$$\chi^{(2)}_{\alpha\beta\gamma}(-2\omega,\omega,\omega) = \frac{e^3}{\tilde{\omega}^3\hbar^2 m^3 V}\sum_{\mathbf{k}}\sum_{nml}\frac{G^{\alpha\beta\gamma}_{nml}(\mathbf{k})}{[\omega_{mn}(\mathbf{k}) - 2\tilde{\omega}]} \times\left[\frac{f_{nl}(\mathbf{k})}{\omega_{ln}(\mathbf{k}) - \tilde{\omega}} + \frac{f_{ml}(\mathbf{k})}{\omega_{ml}(\mathbf{k}) - \tilde{\omega}}\right], \tag{35}$$

with the combination of matrix elements $G^{\alpha\beta\gamma}_{nml}$ defined by

$$G^{\alpha\beta\gamma}_{nml}(\mathbf{k}) = \frac{1}{2i}[p^{\alpha}_{nm}(\mathbf{k})\{p^{\beta}_{ml}(\mathbf{k})p^{\gamma}_{ln}(\mathbf{k})\} + p^{\alpha}_{nm}(-\mathbf{k})\{p^{\beta}_{ml}(-\mathbf{k}) \times p^{\gamma}_{ln}(-\mathbf{k})\}] = \mathrm{Im}[p^{\alpha}_{nm}(\mathbf{k})\{p^{\beta}_{ml}(\mathbf{k})p^{\gamma}_{ln}(\mathbf{k})\}]. \tag{36}$$

This expression is equivalent to Aspnes's formulation of the SHG susceptibility for independent Bloch electrons,[16] provided only completely filled and empty bands are considered.

In the case of cubic symmetry, the above expression can be modified taking into account that only the off-diagonal elements $\chi^{(2)}_{xyz}$ are different from zero. We apply the method of invariants by symmetrizing the $G^{\alpha\beta\gamma}_{nml}$ with respect to the Cartesian directions. Defining

$$M_{nml}(\mathbf{k}) = \frac{1}{6}[G^{xyz}_{nml}(\mathbf{k}) + G^{xzy}_{nml}(\mathbf{k}) + \cdots] \tag{37}$$

one obtains for the imaginary part of the SHG susceptibility ($\omega > 0$)

$$\mathrm{Im}[\chi^{(2)}_{xyz}(-2\omega,\omega,\omega)] = \frac{\pi e^3}{\omega^3\hbar^2 m^3 V}\sum_{vc\mathbf{k}}\Bigg[\sum_{c'} M_{vcc'}(\mathbf{k})\Bigg(\frac{2\delta(\omega_{cv}(\mathbf{k})-2\omega)}{[2\omega_{c'v}(\mathbf{k})-\omega_{cv}(\mathbf{k})]}+\frac{\delta(\omega_{cv}(\mathbf{k})-\omega)[2\omega_{c'v}(\mathbf{k})-\omega_{cv}(\mathbf{k})]}{[2\omega_{cv}(\mathbf{k})-\omega_{c'v}(\mathbf{k})][\omega_{c'v}(\mathbf{k})+\omega_{cv}(\mathbf{k})]}\Bigg)$$
$$\times\sum_{v'} M_{cvv'}(\mathbf{k})\Bigg(\frac{2\delta(\omega_{cv}(\mathbf{k})-2\omega)}{[2\omega_{cv'}(\mathbf{k})-\omega_{cv}(\mathbf{k})]}+\frac{\delta(\omega_{cv}(\mathbf{k})-\omega)[2\omega_{cv'}(\mathbf{k})-\omega_{cv}(\mathbf{k})]}{[2\omega_{cv}(\mathbf{k})-\omega_{cv'}(\mathbf{k})][\omega_{cv'}(\mathbf{k})+\omega_{cv}(\mathbf{k})]}\Bigg)\Bigg], \quad (38)$$

with fully occupied valence bands (v) and empty conduction bands (c). A similar expression, but with an erroneous sign, was used in Ref. 15. It is interesting to note that the two-band term $\chi^{(2)\ \mathrm{two}}_{\alpha\beta\gamma}(-2\omega,\omega,\omega)$ vanishes for cubic symmetry.

D. Excitonic and local-field effects

Usually, the linear optical response is strongly modified by electron-hole attraction (excitonic effects) and local-field effects.[8–10] Much less is known about the impact of electron-hole correlation and exchange on the nonlinear optical properties.[21] This is due to the enormously increased computational effort upon considering the coupling between electron-hole pairs. In the following, we propose a method to include excitonic effects in the calculation of the SHG susceptibility that is based on the time-evolution technique developed earlier by some of the present authors for solving the BSE.[11,12]

In the Bloch picture (24), the inclusion of the screened Coulomb attraction and the short-ranged exchange term requires additional approximations. To simplify the calculation of the expectation values of the creation and annihilation operators in Eq. (26), we neglect dynamical screening effects and the interaction between (v,v') and (c,c') states, which violate the particle conservation, as well as excitations corresponding to negative frequencies.[34] In the case of bulk silicon, it has been numerically shown[36] that the influence of these effects is negligible. The BSE can be reformulated to find the resolvent of a Hermitian (quasi)electron-(quasi)hole Hamiltonian $\hat{H}_{\mathrm{Ex}}$, reduced by the photon energy.[12] This Hamiltonian leads to electron-hole pair states $|\Lambda\rangle$. For vanishing center-of-mass motion,[51] they are given by

$$|\Lambda\rangle = \sum_{vc\mathbf{k}} A^{cv}_{\Lambda}(\mathbf{k})\hat{a}^{\dagger}_{c\mathbf{k}}\hat{a}_{v\mathbf{k}}|g\rangle, \quad (39)$$

where $|g\rangle$ is the ground state of the system and $A^{cv}_{\Lambda}(\mathbf{k})$ are complex mixing coefficients of electron-hole pairs in different single-particle states of the IQA. The eigenvectors $A^{cv}_{\Lambda}(\mathbf{k})$ and the pair excitation energies E_{Λ} solve the eigenvalue problem

$$\sum_{c'v'\mathbf{k}'} \hat{H}_{\mathrm{Ex}}(c,v,\mathbf{k};c',v',\mathbf{k}')A^{c'v'}_{\Lambda}(\mathbf{k}') = E_{\Lambda}A^{cv}_{\Lambda}(\mathbf{k}), \quad (40)$$

where $\hat{H}_{\mathrm{Ex}}$ is the Hermitian resonant part of the complete two-particle Hamiltonian. It is given by

$$\begin{aligned}\hat{H}_{\mathrm{Ex}}(cv\mathbf{k},c'v'\mathbf{k}') &= [\epsilon_c(\mathbf{k})-\epsilon_v(\mathbf{k})]\delta_{cc'}\delta_{vv'}\delta_{\mathbf{kk}'}\\ &- \int d^3\mathbf{x}\int d^3\mathbf{x}'[\phi^*_{c\mathbf{k}}(\mathbf{x})\phi_{v\mathbf{k}}(\mathbf{x}')W(\mathbf{x},\mathbf{x}';0)\\ &\times\phi_{c'\mathbf{k}'}(\mathbf{x})\phi^*_{v'\mathbf{k}'}(\mathbf{x}') - 2\phi^*_{c\mathbf{k}}(\mathbf{x})\phi_{v\mathbf{k}}(\mathbf{x})\overline{v}(\mathbf{x},\mathbf{x}';0)\\ &\times\phi_{c'\mathbf{k}'}(\mathbf{x}')\phi^*_{v'\mathbf{k}'}(\mathbf{x}')], \end{aligned} \quad (41)$$

where W is the statically screened Coulomb potential and $\overline{v}$ represents the bare Coulomb potential without the long-range part.[27,28,31,34] The diagonal first part of the Hamiltonian (41) contains the vertical quasiparticle transition energies $\epsilon_n(\mathbf{k})$. In the explicit computations, we calculate these quasiparticle energies in the *GW* approximation.[5,6,34] The second contribution contains two terms. The first one represents the electron-hole attraction, while the second one represents the short-ranged electron-hole exchange,[37] or, in other words, LF effects.[36] The $\phi_{n\mathbf{k}}(\mathbf{x})$ are quasiparticle wave functions approximated, e.g., by Kohn-Sham orbitals. Using the electron-hole pair states $|\Lambda\rangle$ and their completeness in evaluating Eq. (26), and neglecting intraband contributions, one obtains (see Appendix B)

$$\chi^{(2)}_{\alpha\beta\gamma}(-2\omega;\omega,\omega) = -\frac{ie^3}{2m^3\tilde{\omega}^3 V}\sum_{\mathbf{k},\mathbf{k}',\mathbf{k}''}\sum_{\Lambda\Lambda'}\sum_{cv}\sum_{c_1'v_1'}\Bigg\{ + \frac{p^{\gamma}_{vc}(\mathbf{k})A^{cv}_{\Lambda}(\mathbf{k})p^{\alpha}_{c_1'v_1'}(\mathbf{k}'')(A^{c_1'v_1'}_{\Lambda'})^*(\mathbf{k}'')}{[E_\Lambda+\hbar\tilde{\omega}][E_{\Lambda'}+2\hbar\tilde{\omega}]}$$
$$\times\Bigg[\sum_{c_1c'v_1} p^{\beta}_{c_1c'}(\mathbf{k}')(A^{c_1v_1}_{\Lambda})^*(\mathbf{k}')A^{c'v_1}_{\Lambda'}(\mathbf{k}') - \sum_{v_1v'c_1} p^{\beta}_{v'v_1}(\mathbf{k}')(A^{c_1v_1}_{\Lambda})^*(\mathbf{k}')A^{c_1v'}_{\Lambda'}(\mathbf{k}')\Bigg]$$
$$- \frac{p^{\gamma}_{vc}(\mathbf{k})A^{cv}_{\Lambda}(\mathbf{k})p^{\beta}_{c_1'v_1'}(\mathbf{k}')(A^{c_1'v_1'}_{\Lambda'})^*(\mathbf{k}')}{[E_\Lambda+\hbar\tilde{\omega}][E_\Lambda-E_{\Lambda'}+2\hbar\tilde{\omega}]}$$
$$\times\Bigg[\sum_{c_1c'v_1} p^{\alpha}_{c_1c'}(\mathbf{k}'')(A^{c_1v_1}_{\Lambda})^*(\mathbf{k}'')A^{c'v_1}_{\Lambda'}(\mathbf{k}'') - \sum_{v_1v'c_1} p^{\alpha}_{v'v_1}(\mathbf{k}'')(A^{c_1v_1}_{\Lambda})^*(\mathbf{k}'')A^{c_1v'}_{\Lambda'}(\mathbf{k}'')\Bigg]$$
$$- \frac{p^{\beta}_{vc}(\mathbf{k}')A^{cv}_{\Lambda}(\mathbf{k}')p^{\gamma}_{c_1'v_1'}(\mathbf{k})(A^{c_1'v_1'}_{\Lambda'})^*(\mathbf{k})}{[E_{\Lambda'}-\hbar\tilde{\omega}][E_{\Lambda'}-E_\Lambda-2\hbar\tilde{\omega}]}$$
$$\times\Bigg[\sum_{c_1c'v_1} p^{\alpha}_{c_1c'}(\mathbf{k}'')(A^{c_1v_1}_{\Lambda})^*(\mathbf{k}'')A^{c'v_1}_{\Lambda'}(\mathbf{k}'') - \sum_{v_1v'c_1} p^{\alpha}_{v'v_1}(\mathbf{k}'')(A^{c_1v_1}_{\Lambda})^*(\mathbf{k}'')A^{c_1v'}_{\Lambda'}(\mathbf{k}'')\Bigg]$$
$$+ \frac{p^{\alpha}_{vc}(\mathbf{k}'')A^{cv}_{\Lambda}(\mathbf{k}'')p^{\gamma}_{c_1'v_1'}(\mathbf{k})(A^{c_1'v_1'}_{\Lambda'})^*(\mathbf{k})}{[E_{\Lambda'}-\hbar\tilde{\omega}][E_\Lambda-2\hbar\tilde{\omega}]}$$
$$\times\Bigg[\sum_{c_1c'v_1} p^{\beta}_{c_1c'}(\mathbf{k}')(A^{c_1v_1}_{\Lambda})^*(\mathbf{k}')A^{c'v_1}_{\Lambda'}(\mathbf{k}') - \sum_{v_1v'c_1} p^{\beta}_{v'v_1}(\mathbf{k}')(A^{c_1v_1}_{\Lambda})^*(\mathbf{k}')A^{c_1v'}_{\Lambda'}(\mathbf{k}')\Bigg] + (\beta\leftrightarrow\gamma)\Bigg\}. \quad (42)$$

The calculation of $\chi^{(2)}_{\alpha\beta\gamma}(-2\omega;\omega,\omega)$ according to Eq. (42) seemingly requires the solution of the eigenvalue problem (40) for the exciton Hamiltonian (41). The rank of $\hat{H}_{\mathrm{Ex}}$ is given by the number of states $N=N_v\times N_c\times N_{\mathbf{k}}$, where N_v is the number of valence bands, N_c is the number of conduction bands, and $N_{\mathbf{k}}$ is the number of points used to sample the (BZ). As will be shown below, a high number of $\mathbf{k}$ points are required to obtain numerically converged SHG spectra. This renders the diagonalization of $\hat{H}_{\mathrm{Ex}}$ a computationally very expensive task. In order to bypass the diagonalization bottleneck, we extend an earlier suggestion by Glutsch *et al.*:[38] If the energy dependence of the macroscopic polarizability on the eigenvalues of the exciton Hamiltonian is Fourier transformed, the polarizability can be obtained from the solution of an initial-value problem for the vector

$$\psi^{\beta}_{cv\mathbf{k}}(t) = \sum_{\mathbf{k}}\sum_{c'v'} p^{\beta}_{c'v'}(\mathbf{k}')\sum_{\Lambda} A^{cv}_{\Lambda}(\mathbf{k})(A^{c'v'}_{\Lambda})^*(\mathbf{k}')e^{-(i/\hbar)E_\Lambda t}. \quad (43)$$

The time evolution of this vector is driven by the two-particle Hamiltonian

$$\hat{H}_{\mathrm{Ex}}\psi^{\beta}_{cv\mathbf{k}}(t) = i\hbar\partial_t\psi^{\beta}_{cv\mathbf{k}}(t) \quad (44)$$

and its initial value is given by

$$\psi^{\beta}_{cv\mathbf{k}}(0) = p^{\beta}_{cv\mathbf{k}}. \quad (45)$$

This results in a SHG susceptibility (see Appendix B) of the form

$$\chi^{(2)}_{\alpha\beta\gamma}(-2\omega;\omega,\omega) = \frac{ie^3}{m^3\tilde{\omega}^3 V\hbar^2}\sum_{cv\mathbf{k}}\int_0^\infty \mathrm{d}t\int_0^\infty \mathrm{d}t' e^{i2\tilde{\omega}t}e^{i\tilde{\omega}t'}\mathrm{Re}\Bigg[\sum_{c'}\psi^{\alpha}_{c'v\mathbf{k}}(-t)\{(\psi^{\gamma}_{cv\mathbf{k}})^*(t')\psi^{\beta}_{cc'\mathbf{k}}(0) + (\psi^{\beta}_{cv\mathbf{k}})^*(t')\psi^{\gamma}_{cc'\mathbf{k}}(0)\}$$
$$- \sum_{v'}\psi^{\alpha}_{cv'\mathbf{k}}(-t)\{(\psi^{\gamma}_{cv\mathbf{k}})^*(t')\psi^{\beta}_{v'v\mathbf{k}}(0) + (\psi^{\beta}_{cv\mathbf{k}})^*(t')\psi^{\gamma}_{v'v\mathbf{k}}(0)\}\Bigg] - \int_0^\infty \mathrm{d}t\int_t^\infty \mathrm{d}t' e^{i\tilde{\omega}t}e^{i\tilde{\omega}t'}\mathrm{Re}\Bigg[\sum_{c'}\{\psi^{\beta}_{c'v\mathbf{k}}(t)(\psi^{\gamma}_{cv\mathbf{k}})^*(t')$$
$$+ \psi^{\gamma}_{c'v\mathbf{k}}(t)(\psi^{\beta}_{cv\mathbf{k}})^*(t')\}\psi^{\alpha}_{cc'\mathbf{k}}(0) - \sum_{v'}\{\psi^{\beta}_{cv'\mathbf{k}}(t)(\psi^{\gamma}_{cv\mathbf{k}})^*(t') + \psi^{\gamma}_{cv'\mathbf{k}}(t)(\psi^{\beta}_{cv\mathbf{k}})^*(t')\}\psi^{\alpha}_{v'v\mathbf{k}}(0)\Bigg]. \quad (46)$$

While the time integrations in the first term on the right-hand side (rhs) of Eq. (46) can be performed independently, they cannot be separated in the second part, rendering its evaluation very expensive, because of the order of 10^3 time steps are usually required. Fortunately, it turns out that the second term on the rhs of Eq. (46) is comparatively small for photon energies above the band gap. Within the IPA, this can be seen easily: In this case, the second term reduces to

$$\frac{-e^3}{m^3\tilde{\omega}^2V\hbar^2}\sum_{cv\mathbf{k}}\frac{1}{\omega_{cv}(\mathbf{k})[\omega_{cv}(\mathbf{k})-\tilde{\omega}]} \times\left[\sum_{c'}\frac{G^{\alpha\beta\gamma}_{cc'v}(\mathbf{k})}{\omega_{cv}(\mathbf{k})+\omega_{c'v}(\mathbf{k})}+\sum_{v'}\frac{G^{\alpha\beta\gamma}_{v'vc}(\mathbf{k})}{\omega_{vc}(\mathbf{k})+\omega_{v'c}(\mathbf{k})}\right] \tag{47}$$

and is thus much smaller than the double- and single-frequency contributions, i.e., contributions proportional to

$$\frac{f_{nm}(\mathbf{k})}{\omega_{nm}(\mathbf{k})-2\tilde{\omega}} \tag{48}$$

and

$$\frac{f_{nm}(\mathbf{k})}{\omega_{nm}(\mathbf{k})-\tilde{\omega}} \tag{49}$$

entering the first term on the rhs of Eq. (46). For the case of electron-hole interaction, the small contribution of the second term on the rhs of Eq. (46) is demonstrated numerically in Fig. 1. Due to computational limitations, we used a set of 20 random **k** points to sample the BZ, which is of course not enough for convergence. But it might be enough to indicate how the second term on the rhs of Eq. (46) contributes. This term will be neglected in the following.

As can be seen in Fig. 1, the SHG susceptibility calculated according to Eq. (46) diverges as $\omega\rightarrow 0$. Unfortunately, the replacement of the prefactor $\tilde{\omega}^{-3}$ by energy differences (as in the IQA case) is not possible any more. For this reason (using our time-dependent formalism and finite lifetime broadening of the electron-hole pairs), we are not able to calculate the static limit $\chi^{(2)}_{xyz}(0)$ including excitonic and LF effects. To attack this problem, we would either need to solve the eigenvalue problem (40) and to replace the $\tilde{\omega}^{-3}$ in Eq. (42) by the eigenvalues E_Λ (analogous to the method in Ref. 35, or to follow the method outlined in Ref. 21. As will be shown below, the low-frequency values calculated within our time-evolution approach agree well with the results by Chang *et al.*[21]

III. EXAMPLE: BULK GaAs

A. Computational approach

Due to the availibility of recent experimental data[20] and earlier theoretical work (see, e.g., Refs. 15 and 17–19), we use bulk GaAs as an example to demonstrate the influence of many-body effects on SHG spectra. We start from *first-principles* pseudopotential calculations, using a massively parallel multigrid implementation of the DFT-LDA.[39] The core electrons are eliminated with the use of pseudopotentials.[40] The spacing of the finest mesh used to describe the valence electron wave functions and charge density is 0.246 Å.

In the second step, we include electronic self-energy effects in order to account for the quasiparticle aspects. This requires the replacement of the LDA exchange and correlation potential by the nonlocal and energy-dependent self-energy operator $\Sigma(\mathbf{r},\mathbf{r}';E)$. We calculate Σ in the *GW* approximation,[5,6,34] where it is expressed as a convolution of the single-particle propagator *G* and the dynamically screened Coulomb interaction *W*. As a further approximation, we use a model dielectric function[41] to calculate *W*. This speeds up the calculations substantially. Our approach lifts the underestimation of transition energies. The E_0, E_1, E_0', and E_2 critical point energies of the bulk band structure are blueshifted from 0.6, 2.5, 3.9, and 4.1 eV to 1.4, 3.2, 4.7, and 5.0 eV, respectively. These transition energies are in good agreement with the values of 1.52, 3.04, 4.6–4.8, and 4.9–5.1 eV measured at low temperatures.[42] Alternatively, one can use a rigid shift of 0.6 eV (scissors operator) to improve the agreement between the single-particle energies and experiment. Because this is computationally much cheaper, this option is used in the following for convergence tests. After imposing the quasiparticle corrections upon the DFT-LDA values, one has to rescale the oscillator strengths of the transition matrix elements.[7,14]

Electron-hole attraction and local-field effects are taken into account in the third step. Thereby, the exciton Hamiltonian (41) is calculated using the approach outlined in Ref. 12. In particular, the screened electron-hole attraction *W* is calculated using the same approximations as in the self-energy.[41]

Before we turn to the calculated spectra, we mention one difficulty associated with including the electron-hole attraction effects: The electron-hole pair energies E_Λ do not correspond to the excitation of single electron-hole pairs anymore. Rather, they result from the superposition of many contrib-

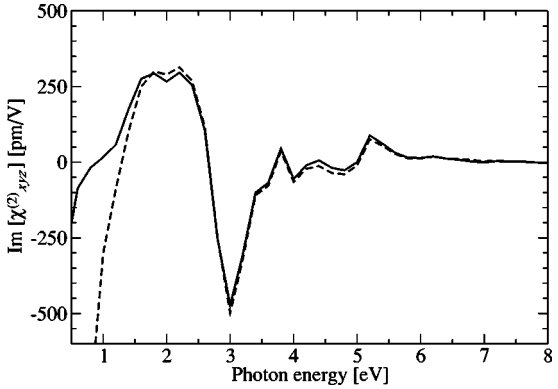

FIG. 1. $\mathrm{Im}[\chi^{(2)}_{xyz}]$ calculated for bulk GaAs using 20 random **k** points. Complete calculations and results obtained by neglecting the second term on the rhs of Eq. (46) are shown by dashed and solid lines, respectively.

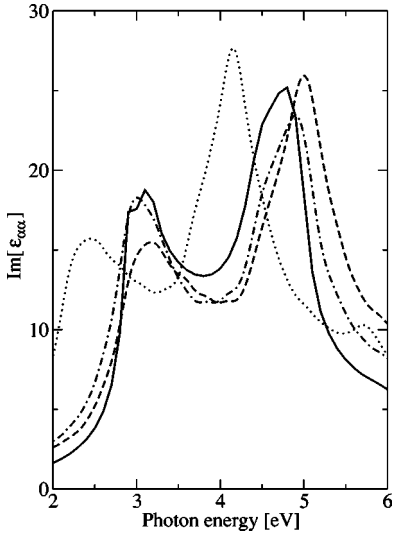

FIG. 2. Imaginary part of the dielectric function for bulk GaAs calculated within the IPA (dotted line), the IQA (dashed line), and by including electron-hole interaction (dashed-dotted line) is compared with measured data (solid line) (Ref. 43).

uting pairs of states. This leads to the question of how the transition matrix elements have to be renormalized. One possibility is to neglect the exciton binding energy and to rescale only with the quasiparticle energies,[7,14]

$$p^{\alpha}_{mn}(\mathbf{k}) \rightarrow \frac{\epsilon^{\mathrm{QP}}_{mn}(\mathbf{k})}{\epsilon^{\mathrm{LDA}}_{mn}(\mathbf{k})} p^{\alpha}_{mn}(\mathbf{k}). \tag{50}$$

Another option consists in rescaling the complete two-particle state with the two-particle energy E_Λ,

$$\sum_{cv\mathbf{k}} p^{\alpha}_{cv}(\mathbf{k})(A^{cv}_{\Lambda})^{*}(\mathbf{k}) \rightarrow \sum_{cv\mathbf{k}} \frac{E_\Lambda}{\epsilon^{\mathrm{LDA}}_{cv}(\mathbf{k})} p^{\alpha}_{cv}(\mathbf{k})(A^{cv}_{\Lambda})^{*}(\mathbf{k}). \tag{51}$$

In numerical tests for the linear optical response, we found only negligible differences between the two methods. In the following, we use Eq. (50) for SHG and Eq. (51) for linear optical spectra.

B. Linear response

The linear optical response of GaAs up to 6 eV is found to be completely converged using 1000 random **k** points in the BZ of the eight-atom supercell (SC) (equivalent to 4000 **k** points in the BZ of the primitive unit cell) and 10 conduction bands. Results for the imaginary part of the dielectric function obtained in the IPA and IQA as well as from the solution of the BSE are compared with experiment[43] in Fig. 2. The IQA and BSE spectra are based on *GW* calculations. We find the IQA spectrum to be blueshifted with respect to the IPA results. Good agreement with experiment is found concerning the energy positions of the E_1, E_0', and E_2 critical points. Solving the BSE for the polarization function leads to a slight redistribution of oscillator strength from E_0' and E_2 to E_1 accompanied by a small redshift. The spectrum calculated on the BSE level of theory agrees well with

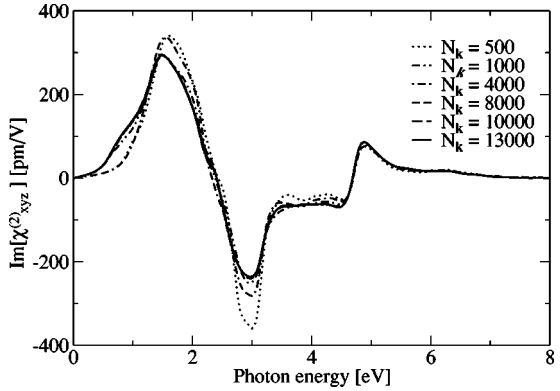

FIG. 3. $\mathrm{Im}[\chi^{(2)}_{xyz}]$ calculated within the IQA (with scissors operator) using different numbers N_k of random **k** points.

experiment[43] and earlier calculations.[44] The relatively small influence of excitonic and local-field effects probably explains the success of calculations of GaAs surface optical properties where many-body effects were neglected or simply approximated by rigidly shifting the conduction-band energies.[45,46]

C. Nonlinear response

The major features of the SHG signal are converged using 500 random **k** points in the BZ of the eight-atom SC. However, to achieve complete numerical convergence, the number of **k** points has to be increased to about 8000 random points in the BZ of the eight-atom SC, as shown in Fig. 3.

In order to establish the accuracy limits of our calculation, we calculated the SHG spectra of Si with 500 random **k** points. Due to the inversion symmetry, bulk Si is expected to show no SHG signal. As can be seen in Fig. 4, the magnitude of the calculated Si SHG susceptibility is indeed more than two orders of magnitude smaller than that of GaAs. It shows the numerical error bar (keeping in mind that we are not explicitly using the inversion symmetry of Si in our approach) and is an impressive proof of the accuracy of our implementation.

Computer time and memory limitations prevented us from studying the effects of electron-hole interactions and local

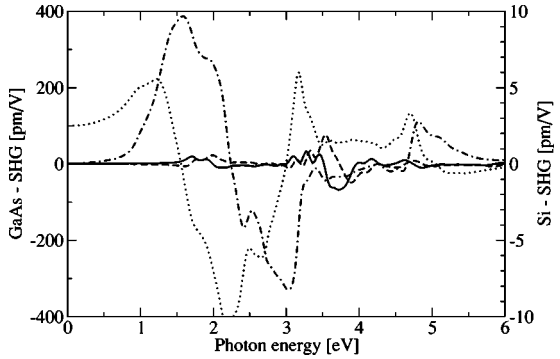

FIG. 4. $\chi^{(2)}_{xyz}$ calculated within the IQA (with scissors operator) using 500 random **k** points for GaAs and Si. The real part for GaAs (Si) is shown by a dotted (solid) line, the imaginary part by a dashed-dotted (dashed) line. Note the different scales.

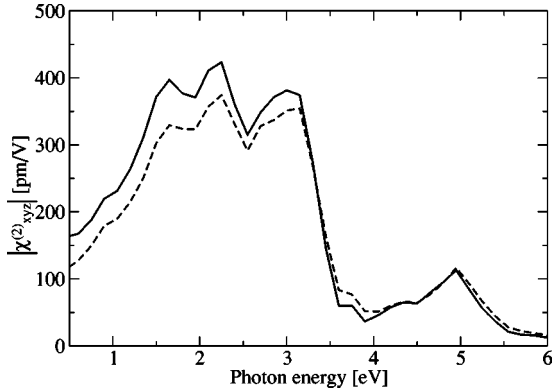

FIG. 5. $|\chi^{(2)}_{xyz}|$ calculated for GaAs within the IQA (dashed line) and by including excitonic and local-field effects (solid line). See text.

fields according to Eq. (46) for more than 500 **k** points. The SHG spectra with and without excitonic effects calculated with these 500 **k** points are shown in Fig. 5. Similar to the study performed by Chang, Shirley, and Levine,[21] we find a rather moderate increase of the SHG susceptibility for energies below about 3 eV (see also Table I).

For higher photon energies, a slight reduction of the susceptibility occurs.

Figure 6 shows a comparison of the SHG spectrum calculated within the IPA, the IQA, and on the BSE level of theory with experimental data.[20] Self-energy effects in the *GW* approximation lead to a blueshift of the IPA results as well as to a redistribution of oscillator strength. Consistent with earlier calculations by Hughes and Sipe,[17] a pronounced underestimation of the predicted peak height compared to the measurement for photon energies of about 1.5 eV is observed. This may correspond to the underestimation of the E_1 peak in the linear absorption spectrum calculated within the IQA. Indeed, we find that the inclusion of electron-hole attraction and local-field effects (by adding the difference between the IQA and BSE results calculated for 500 **k** points) enhances the 1.5 eV peak. The calculated effect, however, is certainly not large enough to fully account for the discrepancies between the IQA results and experiment. One possible reason could be the limited number of **k** points. Due to the mixing of the states related to the exchange interaction and electron-hole attraction, this may impair the quality of the spectrum more than for calculations where only vertical transitions enter. On the other hand, there are also some uncertainties in the experimental determination of the SHG susceptibility, e.g., all surface contributions must be subtracted from the total measured signal to obtain the bulk contribution.

TABLE I. Low-frequency values of $\chi^{(2)}_{xyz}(-2\omega;\omega\omega)$ [pm/V] in comparison with previous calculations.

	$\hbar\omega=0.586$ eV			$\hbar\omega=0.700$ eV		
	IPA	IQA	BSE	IPA	IQA	BSE
Present calculation	270.0	119.5	160.0	309.0	132.5	172.5
Chang *et al.*[21]		123.9	153.4		141.9	179.2

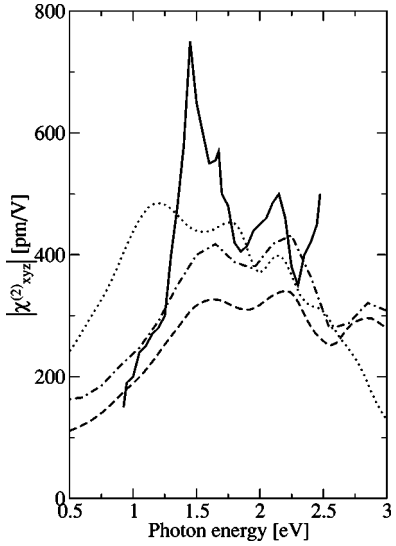

FIG. 6. $|\chi^{(2)}_{xyz}|$ calculated within the IPA (dotted line), the IQA (dashed line), and by including electron-hole attraction (dashed-dotted line) for bulk GaAs with 1000 random **k** in comparison with experiment (solid line) (Ref. 20). *GW* calculations are used to obtain the quasiparticle energies.

IV. CONCLUSIONS

An approach for the calculation of the second-harmonic polarizability has been presented that allows for the inclusion of excitonic effects from *first-principles* over a wide energy range. Numerical results obtained for bulk GaAs show that the inclusion of the electron-hole interaction improves the agreement with experimental data by moderately increasing the SHG susceptibilty for photon energies below about 3 eV. However, the effect is too weak to account completely for the differences between the spectra within the IQA and the measured data available at present.

ACKNOWLEDGMENTS

Grants of computer time from the Leibniz-Rechenzentrum München and the Höchstleistungsrechenzentrum Stuttgart are gratefully acknowledged. The work was financially supported through the EU NANOQUANTA network of excellence (NMP4-CT-2004-500198).

APPENDIX A: COMPARISON WITH THE SIPE FORMALISM

Here we show the equivalence of the expressions (B1)–(B3) from Ref. 17 to our formulation. After correcting a minor misprint (see Ref. 47) and the separation into two- and three-band contributions, one obtains from Ref. 17

$$\chi^{\alpha\beta\gamma}_{II\ \mathrm{three}}(-2\omega,\omega,\omega)=\frac{e^3}{\hbar^2 V}\sum_{\mathbf{k}}\sum_{nml}\frac{r^{\alpha}_{nm}(\mathbf{k})\{r^{\beta}_{ml}(\mathbf{k})r^{\gamma}_{ln}(\mathbf{k})\}}{[\omega_{ln}(\mathbf{k})-\omega_{ml}(\mathbf{k})]}\left[\frac{2f_{nm}}{\omega_{mn}(\mathbf{k})-2\tilde{\omega}}+\frac{f_{ml}}{\omega_{ml}(\mathbf{k})-\tilde{\omega}}+\frac{f_{ln}}{\omega_{ln}(\mathbf{k})-\tilde{\omega}}\right], \tag{A1}$$

$$\eta^{\alpha\beta\gamma}_{II\ \mathrm{three}}(-2\omega,\omega,\omega)=\frac{e^3}{\hbar^2 V}\sum_{\mathbf{k}}\sum_{nml}\left\{\omega_{mn}(\mathbf{k})r^{\alpha}_{nm}(\mathbf{k})\{r^{\beta}_{ml}(\mathbf{k})r^{\gamma}_{ln}(\mathbf{k})\}\left[\frac{f_{nl}}{\omega^2_{ln}(\mathbf{k})[\omega_{ln}(\mathbf{k})-\tilde{\omega}]}--\frac{f_{lm}}{\omega^2_{ml}(\mathbf{k})[\omega_{ml}(\mathbf{k})-\tilde{\omega}]}\right]\right.$$
$$\left.+2\left[\frac{f_{nm}r^{\alpha}_{nm}(\mathbf{k})\{r^{\beta}_{ml}(\mathbf{k})r^{\gamma}_{ln}(\mathbf{k})\}[\omega_{ml}(\mathbf{k})-\omega_{ln}(\mathbf{k})]}{\omega^2_{mn}(\mathbf{k})[\omega_{mn}(\mathbf{k})-2\tilde{\omega}]}\right]\right\}, \tag{A2}$$

$$\frac{i}{2\tilde{\omega}}\sigma^{\alpha\beta\gamma}_{II\ \mathrm{three}}(-2\omega,\omega,\omega)=\frac{e^3}{\hbar^2 2V}\left\{\sum_{\mathbf{k}}\sum_{nml}\frac{f_{nm}}{\omega^2_{mn}(\mathbf{k})[\omega_{mn}(\mathbf{k})-\tilde{\omega}]}[\omega_{nl}(\mathbf{k})r^{\alpha}_{lm}(\mathbf{k})\{r^{\beta}_{mn}(\mathbf{k})r^{\gamma}_{nl}(\mathbf{k})\}-\omega_{lm}(\mathbf{k})r^{\alpha}_{nl}(\mathbf{k})\{r^{\beta}_{lm}(\mathbf{k})r^{\gamma}_{mn}(\mathbf{k})\}]\right\}, \tag{A3}$$

$$\eta^{abc}_{II\ \mathrm{two}}(-2\tilde{\omega},\tilde{\omega},\tilde{\omega})=-\frac{8ie^3}{\hbar^2 V}\sum_{\mathbf{k}}\sum_{nm}\frac{f_{nm}r^{\alpha}_{nm}(\mathbf{k})}{\omega^2_{mn}(\mathbf{k})[\omega_{mn}(\mathbf{k})-2\tilde{\omega}]}\{\Delta^{\beta}_{mn}(\mathbf{k})r^{\gamma}_{mn}(\mathbf{k})\}, \tag{A4}$$

$$\frac{i}{2\tilde{\omega}}\sigma^{\alpha\beta\gamma}_{II\ \mathrm{two}}(-2\omega,\omega,\omega)=-\frac{ie^3}{\hbar^2 2V}\sum_{\mathbf{k}}\sum_{nm}\frac{f_{nm}r^{\alpha}_{nm}(\mathbf{k})}{\omega^2_{mn}(\mathbf{k})[\omega_{mn}(\mathbf{k})-\tilde{\omega}]}\{\Delta^{\gamma}_{mn}(\mathbf{k})r^{\beta}_{mn}(\mathbf{k})\}. \tag{A5}$$

The dipole matrix elements $r^{\alpha}_{mn}(\mathbf{k})$ are defined as[14]

$$r^{\alpha}_{mn}(\mathbf{k})=\begin{cases}\dfrac{p^{\alpha}_{mn}(\mathbf{k})}{im\omega_{mn}(\mathbf{k})}: & \epsilon_m(\mathbf{k})\neq\epsilon_n(\mathbf{k})\\ 0: & \epsilon_n(\mathbf{k})=\epsilon_m(\mathbf{k}).\end{cases} \tag{A6}$$

We collect all three-band contributions via

$$\chi^{(2)\ \mathrm{three}}_{\alpha\beta\gamma}=\chi^{\alpha\beta\gamma}_{II\ \mathrm{three}}+\eta^{\alpha\beta\gamma}_{II\ \mathrm{three}}+\frac{i}{2\tilde{\omega}}\sigma^{\alpha\beta\gamma}_{II\ \mathrm{three}} \tag{A7}$$

and we obtain

$$\chi^{(2)\ \mathrm{three}}_{\alpha\beta\gamma}(-2\omega,\omega,\omega)=\frac{e^3}{\hbar^2 V}\sum_{\mathbf{k}}\sum_{nml}\frac{f_{ml}r^{\alpha}_{nm}(\mathbf{k})\{r^{\beta}_{ml}(\mathbf{k})r^{\gamma}_{ln}(\mathbf{k})\}}{\omega_{ml}(\mathbf{k})-\tilde{\omega}}\left[\frac{1}{[\omega_{ln}(\mathbf{k})-\omega_{ml}(\mathbf{k})]}+\frac{\omega_{mn}(\mathbf{k})}{\omega^2_{ml}(\mathbf{k})}-\frac{1}{2}\frac{\omega_{ln}(\mathbf{k})}{\omega^2_{ml}(\mathbf{k})}\right]+\frac{f_{ln}r^{\alpha}_{nm}(\mathbf{k})\{r^{\beta}_{ml}(\mathbf{k})r^{\gamma}_{ln}(\mathbf{k})\}}{\omega_{ln}(\mathbf{k})-\tilde{\omega}}$$
$$\times\left[\frac{1}{[\omega_{ln}(\mathbf{k})-\omega_{ml}(\mathbf{k})]}-\frac{\omega_{mn}(\mathbf{k})}{\omega^2_{ln}(\mathbf{k})}+\frac{1}{2}\frac{\omega_{ml}(\mathbf{k})}{\omega^2_{ln}(\mathbf{k})}\right]+\frac{2f_{nm}r^{\alpha}_{nm}(\mathbf{k})\{r^{\beta}_{ml}(\mathbf{k})r^{\gamma}_{ln}(\mathbf{k})\}}{\omega_{mn}(\mathbf{k})-2\tilde{\omega}}$$
$$\times\left[\frac{1}{[\omega_{ln}(\mathbf{k})-\omega_{ml}(\mathbf{k})]}+\frac{[\omega_{ml}(\mathbf{k})-\omega_{ln}(\mathbf{k})]}{\omega^2_{mn}(\mathbf{k})}\right]. \tag{A8}$$

Using the definition of the $r^{\alpha}_{nm}(\mathbf{k})$ in Eq. (A6), one sees that this expression is (except for a factor 2 related to the spin degeneracy) equivalent to the three-band contribution (32). In the same way, one can show the equivalence for the two-band contributions.

APPENDIX B: INCLUSION OF COULOMB CORRELATION

Evaluating Eqs. (25) and (26), terms such as

$$\langle a^{\dagger}_{n\mathbf{k}}(0)a_{m\mathbf{k}}(0)a^{\dagger}_{n'\mathbf{k}'}(\tau)a_{m'\mathbf{k}'}(\tau)\rangle_{\mathrm{irred}} \tag{B1}$$

and

$$\langle a^{\dagger}_{n\mathbf{k}}(\tau')a_{n'\mathbf{k}}(\tau')a^{\dagger}_{l\mathbf{k}'}(\tau)a_{l'\mathbf{k}'}(\tau)a^{\dagger}_{m\mathbf{k}''}(0)\hat{a}_{m'\mathbf{k}''}(0)\rangle_{\mathrm{irred}} \tag{B2}$$

appear. Using the completeness of the two-particle-states $|\Lambda\rangle$ and focusing only on the irreducible contributions, one can rewrite them in the form

$$\sum_{\Lambda}\langle \mathrm{g}|a^{\dagger}_{n\mathbf{k}}(0)a_{m\mathbf{k}}(0)|\Lambda\rangle_{\mathrm{irred}}\langle\Lambda|a^{\dagger}_{n'\mathbf{k}'}(\tau)a_{m'\mathbf{k}'}(\tau)|\mathrm{g}\rangle_{\mathrm{irred}} \tag{B3}$$

and

$$\sum_{\Lambda\Lambda'} \langle \mathrm{g}|a^{\dagger}_{n\mathbf{k}}(\tau')a_{n'\mathbf{k}}(\tau')|\Lambda\rangle_{\mathrm{irred}}\langle\Lambda|a^{\dagger}_{l\mathbf{k}'}(\tau)a_{l'\mathbf{k}'}(\tau)|\Lambda'\rangle_{\mathrm{irred}} \times\langle\Lambda'|a^{\dagger}_{m\mathbf{k}''}(0)\hat{a}_{m'\mathbf{k}''}(0)|\mathrm{g}\rangle_{\mathrm{irred}}, \tag{B4}$$

respectively. Here $|\mathrm{g}\rangle$ is the ground state of the system. Using the explicit time dependence of the two-particle states according to Eq. (44), we find

$$\begin{aligned}
&\langle[a^{+}_{n,\mathbf{k}}(t')a_{n',\mathbf{k}}(t'),[a^{+}_{l,\mathbf{k}}(t)a_{l',\mathbf{k}}(t),a^{+}_{m,\mathbf{k}}(0)a_{m',\mathbf{k}}(0)]]\rangle_{\mathrm{irred}}\\
&\quad=\sum_{\Lambda\Lambda'} e^{-(i/\hbar)E_{\Lambda}t'}e^{(i/\hbar)(E_{\Lambda}-E_{\Lambda'})t}\langle \mathrm{g}|a^{+}_{n,\mathbf{k}}a_{n',\mathbf{k}}|\Lambda\rangle_{\mathrm{irred}}\langle\Lambda|a^{+}_{l,\mathbf{k}}a_{l',\mathbf{k}}|\Lambda'\rangle_{\mathrm{irred}}\langle\Lambda'|a^{+}_{m,\mathbf{k}}a_{m',\mathbf{k}}|\mathrm{g}\rangle_{\mathrm{irred}}\\
&\qquad- e^{-(i/\hbar)E_{\Lambda}t'}e^{(i/\hbar)E_{\Lambda'}t}\langle \mathrm{g}|a^{+}_{n,\mathbf{k}}a_{n',\mathbf{k}}|\Lambda\rangle_{\mathrm{irred}}\langle\Lambda|a^{+}_{m,\mathbf{k}}a_{m',\mathbf{k}}|\Lambda'\rangle_{\mathrm{irred}}\langle\Lambda'|a^{+}_{l,\mathbf{k}}a_{l',\mathbf{k}}|\mathrm{g}\rangle_{\mathrm{irred}}\\
&\qquad- e^{-(i/\hbar)E_{\Lambda}t}e^{(i/\hbar)E_{\Lambda'}t'}\langle \mathrm{g}|a^{+}_{l,\mathbf{k}}a_{l',\mathbf{k}}|\Lambda\rangle_{\mathrm{irred}}\langle\Lambda|a^{+}_{m,\mathbf{k}}a_{m',\mathbf{k}}|\Lambda'\rangle_{\mathrm{irred}}\langle\Lambda'|a^{+}_{n,\mathbf{k}}a_{n',\mathbf{k}}|\mathrm{g}\rangle_{\mathrm{irred}}\\
&\qquad+ e^{(i/\hbar)E_{\Lambda'}t'}e^{(i/\hbar)(E_{\Lambda}-E_{\Lambda'})t}\langle \mathrm{g}|a^{+}_{m,\mathbf{k}}a_{m',\mathbf{k}}|\Lambda\rangle_{\mathrm{irred}}\langle\Lambda|a^{+}_{l,\mathbf{k}}a_{l',\mathbf{k}}|\Lambda'\rangle_{\mathrm{irred}}\langle\Lambda'|a^{+}_{n,\mathbf{k}}a_{n',\mathbf{k}}|\mathrm{g}\rangle_{\mathrm{irred}}.
\end{aligned} \tag{B5}$$

In the next step, we apply the relations for the independent quasiparticles in completely filled (v) or empty (c) bands,

$$\langle a^{\dagger}_{v,\mathbf{k}}a_{c,\mathbf{k}}a^{\dagger}_{l,\mathbf{k}'}a_{m,\mathbf{k}'}\rangle_{\mathrm{irred}} = \delta_{lc}\delta_{vm}\delta_{\mathbf{k}\mathbf{k}'}, \tag{B6}$$

$$\langle a^{\dagger}_{l,\mathbf{k}}a_{m,\mathbf{k}}a^{\dagger}_{c,\mathbf{k}'}a_{v,\mathbf{k}'}\rangle_{\mathrm{irred}} = \delta_{mc}\delta_{vl}\delta_{\mathbf{k}\mathbf{k}'}, \tag{B7}$$

and

$$\langle a^{\dagger}_{v,\mathbf{k}}a_{c,\mathbf{k}}a^{\dagger}_{l,\mathbf{k}'}a_{m,\mathbf{k}'}a^{\dagger}_{c',\mathbf{k}''}a_{v',\mathbf{k}''}\rangle_{\mathrm{irred}} = \delta_{\mathbf{k}\mathbf{k}'}\delta_{\mathbf{k}'\mathbf{k}''}(\delta_{vv'}\delta_{lc}\delta_{mc'} - \delta_{cc'}\delta_{lv}\delta_{mv}), \tag{B8}$$

where we have neglected a (three-band-)intraband contribution $\delta_{vv'}\delta_{cc'}\delta_{lm}$ (which vanishes in the IQA). That means we only take into account the processes which already occur in the independent-quasiparticle framework. Additional SHG processes, which would be induced by the Coulomb correlation of electrons and holes, are neglected. In crystals with extended states, they are small. For systems with strongly localized states and weak screening, this approximation needs to be verified. From Eqs. (B6)–(B8) and (26) and accounting for spin degeneracy, we obtain

$$\begin{aligned}
\chi^{(2)}_{\alpha\beta\gamma}(-2w;w,w) = \frac{ie^3}{2m^3\tilde{w}^3V\hbar^2}&\sum_{\mathbf{q},\mathbf{q}',\mathbf{q}''}\sum_{\mathbf{k},\mathbf{k}'}\sum_{\mathbf{k}_1,\mathbf{k}_1'}\sum_{\Lambda\Lambda'}\sum_{c_1'v_1'}\sum_{c'v'}\sum_{c_1v_1}\sum_{cv}\sum_{l'm'n'}\sum_{lmn}\int_{-\infty}^{0}\mathrm{d}t\int_{-\infty}^{t}\mathrm{d}t'\\
&\times e^{-i\tilde{w}(t+t')}A^{cv}_{\Lambda}(\mathbf{k})A^{c'v'}_{\Lambda'}(\mathbf{k}')(A^{c_1v_1}_{\Lambda})^{*}(\mathbf{k}_1)(A^{c_1'v_1'}_{\Lambda'})^{*}(\mathbf{k}_1')[p^{\gamma}_{nn'}(\mathbf{q})p^{\beta}_{ll'}(\mathbf{q}')\\
&+ p^{\beta}_{nn'}(\mathbf{q})p^{\gamma}_{ll'}(\mathbf{q}')]p^{\alpha}_{mm'}(\mathbf{q}'')\times\Big\{e^{-(i/\hbar)E_{\Lambda}t'}e^{(i/\hbar)(E_{\Lambda}-E_{\Lambda'})t}\delta_{n'c}\delta_{nv}\delta_{\mathbf{q}\mathbf{k}}\delta_{mc_1'}\delta_{m'v_1'}\delta_{\mathbf{q}''\mathbf{k}_1'}\delta_{\mathbf{k}_1\mathbf{k}'}\delta_{\mathbf{q}'\mathbf{k}'}[\delta_{v_1v'}\delta_{lc_1}\delta_{l'c'}\\
&- \delta_{c_1c'}\delta_{lv'}\delta_{l'v_1}] - e^{-(i/\hbar)E_{\Lambda}t'}e^{(i/\hbar)E_{\Lambda'}t}\delta_{n'c}\delta_{nv}\delta_{\mathbf{q}\mathbf{k}}\delta_{lc_1'}\delta_{l'v_1'}\delta_{\mathbf{q}''\mathbf{k}_1}\delta_{\mathbf{k}_1\mathbf{k}'}\delta_{\mathbf{q}'\mathbf{k}_1'}[\delta_{v_1v'}\delta_{mc_1}\delta_{m'c'} - \delta_{c_1c'}\delta_{mv'}\delta_{m'v_1}]\\
&- e^{-(i/\hbar)E_{\Lambda}t}e^{(i/\hbar)E_{\Lambda'}t'}\delta_{l'c}\delta_{lv}\delta_{\mathbf{q}'\mathbf{k}}\delta_{nc_1'}\delta_{n'v_1'}\delta_{\mathbf{q}''\mathbf{k}'}\delta_{\mathbf{k}_1\mathbf{k}'}\delta_{\mathbf{q}\mathbf{k}_1'}[\delta_{v_1v'}\delta_{mc_1}\delta_{m'c'} - \delta_{c_1c'}\delta_{mv'}\delta_{m'v_1}]\\
&+ e^{(i/\hbar)(E_{\Lambda}-E_{\Lambda'})t}e^{(i/\hbar)E_{\Lambda'}t'}\delta_{m'c}\delta_{mv}\delta_{\mathbf{q}'\mathbf{k}_1}\delta_{nc_1'}\delta_{n'v_1'}\delta_{\mathbf{q}''\mathbf{k}}\delta_{\mathbf{k}_1\mathbf{k}'}\delta_{\mathbf{q}\mathbf{k}_1'}[\delta_{v_1v'}\delta_{lc_1}\delta_{l'c'} - \delta_{c_1c'}\delta_{lv'}\delta_{l'v_1}]\Big\}.
\end{aligned} \tag{B9}$$

Performing the time integrations in Eq. (B9), one obtains expression (42). On the other hand, we can replace the occurring coefficients $A^{cv}_{\Lambda}(\mathbf{k})$ by the vectors $\psi^{\alpha}_{cv\mathbf{k}}(t)$ according to the definition (43) and obtain the SHG susceptibility in the time-dependent scheme,

$$\chi^{(2)}_{\alpha\beta\gamma}(-2\omega,\omega,\omega) = \frac{ie^3}{2m^3\tilde{\omega}^3V\hbar^2}\sum_{cv\mathbf{k}}\int_0^\infty \mathrm{d}t\int_t^\infty \mathrm{d}t' e^{i\tilde{\omega}(t+t')}\times\Bigg\{\Bigg[\sum_{c'}\psi^{\alpha}_{c'v\mathbf{k}}(-t)(\psi^{\gamma}_{cv\mathbf{k}})^*(t'-t)\psi^{\beta}_{cc'\mathbf{k}}(0) - \psi^{\beta}_{c'v\mathbf{k}}(t)(\psi^{\gamma}_{cv\mathbf{k}})^*(t')\psi^{\alpha}_{cc'\mathbf{k}}(0)$$
$$- \psi^{\gamma}_{c'v\mathbf{k}}(t')(\psi^{\beta}_{cv\mathbf{k}})^*(t)\psi^{\alpha}_{cc'\mathbf{k}}(0) + \psi^{\gamma}_{c'v\mathbf{k}}(t'-t)(\psi^{\alpha}_{cv\mathbf{k}})^*(-t)\psi^{\beta}_{cc'\mathbf{k}}(0) - \sum_{v'}\psi^{\alpha}_{cv'\mathbf{k}}(-t)(\psi^{\gamma}_{cv\mathbf{k}})^*(t'-t)\psi^{\beta}_{vv'\mathbf{k}}(0)$$
$$- \psi^{\beta}_{cv'\mathbf{k}}(t)(\psi^{\gamma}_{cv\mathbf{k}})^*(t')\psi^{\alpha}_{vv'\mathbf{k}}(0) - \psi^{\gamma}_{cv'\mathbf{k}}(t')(\psi^{\beta}_{cv\mathbf{k}})^*(t)\psi^{\alpha}_{vv'\mathbf{k}}(0) + \psi^{\gamma}_{cv'\mathbf{k}}(t'-t)(\psi^{\alpha}_{cv\mathbf{k}})^*(-t)\psi^{\beta}_{vv'\mathbf{k}}(0)\Bigg] + (\beta\leftrightarrow\gamma)\Bigg\}. \tag{B10}$$

Equation (B10) can be further simplified by adding the occurring complex conjugated terms, e.g.,

$$\psi^{\alpha}_{c'v\mathbf{k}}(-t)(\psi^{\gamma}_{cv\mathbf{k}})^*(t'-t)\psi^{\beta}_{cc'\mathbf{k}}(0) + \psi^{\gamma}_{c'v\mathbf{k}}(t'-t)(\psi^{\alpha}_{cv\mathbf{k}})^*(-t)\psi^{\beta}_{cc'\mathbf{k}}(0) = 2\,\mathrm{Re}[\psi^{\alpha}_{c'v\mathbf{k}}(-t)(\psi^{\gamma}_{cv\mathbf{k}})^*(t'-t)\psi^{\beta}_{cc'\mathbf{k}}(0)]. \tag{B11}$$

Finally, after a simple change of the integration variables, we obtain Eq. (46).

*Electronic address: roman@ifto.physik.uni-jena.de

[1] D. E. Aspnes, Solid State Commun. **101**, 85 (1997).
[2] W. Richter and J. T. Zettler, Appl. Surf. Sci. **101**, 465 (1996).
[3] W. G. Schmidt *et al.*, J. Phys.: Condens. Matter **16**, S4323 (2004).
[4] M. C. Downer, B. S. Mendoza, and V. I. Gavrilenko, Surf. Interface Anal. **31**, 966 (2001).
[5] M. S. Hybertsen and S. G. Louie, Phys. Rev. Lett. **55**, 1418 (1985).
[6] R. W. Godby, M. Schlüter, and L. J. Sham, Phys. Rev. Lett. **56**, 2415 (1986).
[7] R. Del Sole and R. Girlanda, Phys. Rev. B **48**, 11 789 (1993).
[8] S. Albrecht, L. Reining, R. Del Sole, and G. Onida, Phys. Rev. Lett. **80**, 4510 (1998).
[9] L. X. Benedict, E. L. Shirley, and R. B. Bohn, Phys. Rev. Lett. **80**, 4514 (1998).
[10] M. Rohlfing and S. G. Louie, Phys. Rev. Lett. **81**, 2312 (1998).
[11] P. H. Hahn, W. G. Schmidt, and F. Bechstedt, Phys. Rev. Lett. **88**, 016402 (2002).
[12] W. G. Schmidt, S. Glutsch, P. H. Hahn, and F. Bechstedt, Phys. Rev. B **67**, 085307 (2003).
[13] P. H. Hahn, W. G. Schmidt, K. Seino, M. Preuss, F. Bechstedt, and J. Bernholc, Phys. Rev. Lett. **94**, 037404 (2005).
[14] J. E. Sipe and E. Ghahramani, Phys. Rev. B **48**, 11 705 (1993).
[15] B. Adolph and F. Bechstedt, Phys. Rev. B **57**, 6519 (1998).
[16] D. E. Aspnes, Phys. Rev. B **6**, 4648 (1972).
[17] J. L. P. Hughes and J. E. Sipe, Phys. Rev. B **53**, 10 751 (1996).
[18] C. Aversa and J. E. Sipe, Phys. Rev. B **57**, 3905 (1998).
[19] W. G. Schmidt, K. Seino, P. Hahn, F. Bechstedt, W. Lu, S. Wang, and J. Bernholc, Thin Solid Films **455/456**, 764 (2004).
[20] S. Bergfeld and W. Daum, Phys. Rev. Lett. **90**, 036801 (2003).
[21] E. K. Chang, E. L. Shirley, and Z. H. Levine, Phys. Rev. B **65**, 035205 (2002).
[22] N. Arzate and B. S. Mendoza, Phys. Rev. B **63**, 113303 (2001).
[23] G. D. Powell, J.-F. Wang, and D. E. Aspnes, Phys. Rev. B **65**, 205320 (2002).
[24] H. Puff, *Einführung in die Allgemeine Theorie der Otischen Eigenschaften von Festkörpern* (Zentralinstitut für Elektronenphysik der Deutschen Akademie der Wissenschaften zu Berlin, Abteilung Theoretische Physik, 1969).
[25] W. Bardyszewski and D. Yevick, Phys. Rev. B **39**, 10 839 (1989).
[26] G. Strinati, Riv. Nuovo Cimento **11**, 1 (1988).
[27] L. J. Sham and T. M. Rice, Phys. Rev. **144**, 708 (1966).
[28] W. Hanke and L. J. Sham, Phys. Rev. B **21**, 4656 (1980).
[29] S. L. Adler, Phys. Rev. **126**, 413 (1962).
[30] N. Wiser, Phys. Rev. **129**, 62 (1963).
[31] W. Hanke and L. J. Sham, Phys. Rev. B **12**, 4501 (1975).
[32] N. Bloembergen, *Nonlinear Optics*, 4th ed. (World Scientific, Singapore, 1996).
[33] P. N. Butcher and D. Cotter, *The Elements of Nonlinear Optics* (Cambridge University Press, Cambridge, 1990).
[34] G. Onida, L. Reining, and A. Rubio, Rev. Mod. Phys. **74**, 601 (2002).
[35] E. Ghahramani, D. J. Moss, and J. E. Sipe, Phys. Rev. B **43**, 8990 (1991).
[36] S. Albrecht, Ph.D. thesis, École Polytechnique, Paris (1999).
[37] F. Bechstedt, W. G. Schmidt, and P. Hahn, Phys. Status Solidi A **188**, 1383 (2001).
[38] S. Glutsch, D. S. Chemla, and F. Bechstedt, Phys. Rev. B **54**, 11 592 (1996).
[39] E. L. Briggs, D. J. Sullivan, and J. Bernholc, Phys. Rev. B **54**, 14 362 (1996).
[40] D. R. Hamann, Phys. Rev. B **40**, 2980 (1989).
[41] F. Bechstedt, R. Del Sole, G. Cappellini, and L. Reining, Solid State Commun. **84**, 765 (1992).
[42] P. Lautenschlager, M. Garriga, S. Logothetidis, and M. Cardona, Phys. Rev. B **35**, 9174 (1987).
[43] D. E. Aspnes and A. A. Studna, Phys. Rev. B **27**, 985 (1983).
[44] L. X. Benedict, E. L. Shirley, and R. B. Bohn, Phys. Rev. B **57**, R9385 (1998).
[45] W. G. Schmidt, F. Bechstedt, W. Lu, and J. Bernholc, Phys. Rev. B **66**, 085334 (2002).

[46] F. Arciprete, C. Goletti, E. Placidi, C. Hogan, P. Chiaradia, M. Fanfoni, F. Patella, and A. Balzarotti, Phys. Rev. B **69**, 081308(R) (2004).

[47] S. Sharma, J. K. Dewhurst, and C. Ambrosch-Draxl, Phys. Rev. B **67**, 165332 (2003).

[48] In the IPA/IQA, the gauge invariance of the response functions can be shown for cold semiconductor materials.[35] However, by employing excitonic and local-field effects, the gauge invariance is broken.

[49] Evaluating the occurring expectation values, one has to use only irreducible diagrams (usually ladder diagrams), which cannot be separated by cutting one interaction line. This problem is discussed in Ref. 25 on p. 10 840 after Eq. (11) or in Ref. 26 on p. 9 and appendix C.

[50] One word of caution is in order here: In the quasiparticle approach, one solves in principle an eigenvalue problem of a non-Hermitian self-energy operator, leading to complex eigenvalues. Strictly speaking, this violates the gauge invariance. However, in most cases only the real parts of the self-energy corrections are considered for practical calculations. This means that the derivation of Ref. 35 remains valid and gauge invariance is formally sustained.

[51] Due to the vanishing photon wave vector, we have no momentum transfer.